Deep–Sea Research I 185 (2022) 103775

Contents lists available at ScienceDirect

Deep-Sea Research Part I

journal homepage: www.elsevier.com/locate/dsri

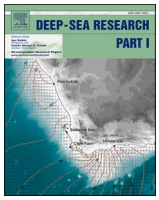

Population structure of *Asconema setubalense* Kent, 1870 at Concepción Seamount, Canary Islands (Spain). Methodological approach using non-invasive techniques

Laura Martín-García [a,*], Elena Prado [b], Jesús M. Falcón [a], Marcos González Porto [a], Antonio Punzón [b], Pablo Martín-Sosa [a]

[a] Centro Oceanográfico de Canarias, Instituto Español de Oceanografía-CSIC, Calle Farola del Mar, nº 22, 38180, Dársena Pesquera, S/C Tenerife, Canarias, Spain
[b] Centro Oceanográfico de Santander, Instituto Español de Oceanografía-CSIC, Promontorio San Martín s/n, 39004, Santander, Cantabria, Spain

ARTICLE INFO

Keywords:
Deep-sea sponge
Structure size
Seamount
Towed vehicle
Sites of community importance

ABSTRACT

The hexactinellid sponge *Asconema setubalense* Kent, 1870is a large bathyal species of the North Atlantic Ocean with a funnel-like body and very large osculum. Populations of *A. setubalense* have a three-dimensional structure and increase the complexity and biodiversity in their habitat, and are therefore considered to be a habitat-forming species. Nevertheless, at present the information on the extension, biomass, density, population structure, and ecology of this species is scarce, and it could be susceptible to the longline fishing practices that take place in the Canary Islands.

The main objectives of this study are to define a functional and accurate methodology to measure specimens of *A. setubalense* by comparing differences in users, techniques, and morphometric measurements; to describe the height-size relationship; to present the population size structure of the species, and to establish a relationship between the size of *A. setubalense* and the environmental variables that can be found at the "Banco de La Concepción" seamount (BC). The obtained results suggest that surface area is the most reliable measurement to define the size of this species, whilst also showing a clear correlation with the height of the species. The selected methodology has made it possible to measure the surface area of 1035 specimens and thus obtain the size structure of the population of *A. setubalense* in BC. The GAM model that was used to analyse the relationship between the size of *A. setubalense* and the geomorphologic variables of BC, shows areas where there is a high probability of finding large specimens of the species. The results of this study greatly enhance the knowledge of this species and its habitat, and should be considered in future conservation directives, or in the development of indicators to show the good environmental state of habitats. Additionally, the study improves analysis methodology that, with the appropriate morphometric measurements, can favour the development of future studies of this species, and indeed others with a similar morphology or growth pattern.

1. Introduction

The hexactinellid sponges of the genus *Asconema* Kent, 1870(Family Rossellidae), are bathyal species (Tabachnick and Menshenina, 2007) that can be found on the hard-bottom habitats of the North Atlantic and Arctic Ocean shelf and seamounts (Gomes-Pereira et al., 2017; Sánchez et al., 2017; Serrano et al., 2017b). They are a large species (up to 1 m in height) with a funnel-like body and a very large osculum. Their population has a three-dimensional structure and increases the complexity and biodiversity of their habitat, therefore *Asconema* can be considered to be representative of a habitat-forming species of European cold-water habitats (Beazley et al., 2013; Davies et al., 2017). Currently, deep-sea sponge aggregations are listed as a type of Vulnerable Marine Ecosystem-VME (UNGA Resolution 61/105) and have been included in the OSPAR list of threatened and/or declining species and habitats in the northeast Atlantic (OSPAR, 2008). In this sense, *Asconema setubalense* Kent, 1870 is a slow-growing organism which makes it particularly vulnerable to human activities such as bottom trawling (Kenchington

Abbreviations: BC, Banco de La Concepción seamount; SCI, Site of Community Importance; ROTV, Remotely Operated Towed Vehicle.

* Corresponding author.
E-mail address: laura.martin@ieo.csic.es (L. Martín-García).

https://doi.org/10.1016/j.dsr.2022.103775
Received 18 May 2021; Received in revised form 6 April 2022; Accepted 8 April 2022
Available online 12 April 2022

et al., 2014; Pusceddu et al., 2014; Victorero et al., 2018; Prado et al., 2021). Thus, the development of management plans for the conservation of these habitats is essential, especially in protected areas.

According to Tabachnick and Menshenina (2007) *A. setubalense* (Fig. 1) is the southernmost representative of the genus, and can be found from the coasts of Spain and Portugal to the Western Sahara at a depth range of 1–2075 m, although the main populations are found at a depth of between 100 and 500 m depth (García-Alegre et al., 2014; Sánchez et al., 2009, 2017). It can live on sandy or muddy bottoms (Sitjà et al., 2019), or rocks with a high percentage of sediment cover (Sánchez et al., 2017), but its growth seems to depend on the presence of hard substrata (Davies et al., 2017; De la Torriente et al., 2018). Despite the importance of this species, at present information regarding the extension, biomass, density, population structure and ecology of this species is limited. Acquiring information on deep-sea sponges is complex and depends on multidisciplinary research surveys aboard large vessels, where direct samplers (dredges and trawls), and indirect ones (e.g., ROVs), are used to study macrofauna. The information gathered on benthic biodiversity in these studies is usually used to describe and map the habitat and the environmental conditions for the growth of deep-sea species (Harris and Baker, 2012; Davies et al., 2015; Sánchez et al., 2017; Serrano et al., 2017a; De la Torriente et al., 2018). Recently, the use of videos and photographic devices have resulted in this information being applied to other areas, such as estimating the size and growth rates of *Asconema setubalense* (Prado et al., 2021). However, until now, there has been no previous study on the population size structure of *A. setubalense* and its relationship with environmental parameters.

Nowadays, indirect sampling methods based on images are a preferable option as they compile a lot of reliable data on marine biodiversity and seafloor geomorphology, whilst being less invasive and having a minor impact on the environment (Bell et al., 2017; Cuvelier et al., 2012). Commonly, cameras mounted on a sled, or a towed vehicle, have an obliquely forward-facing angle of (45°), hampering the scaling of the obtained images and making it difficult to get reliable data on the size of the individuals of most species (Kazanidis et al., 2019). Collected images with these techniques, whenever a scale was provided, have been used in 2D morphometric analysis of sponges in several studies (Barthel et al., 1996; Bo et al., 2012; Bell et al., 2017; Santín et al., 2019). However, these studies did not consider any possible measurement errors produced by the technique, or even the user, or contemplate which kind of morphometric measure may be more reliable for a certain species. The latest advances in this field (morphometric measurements via image analysis) are employed in the 3D reconstruction of the study area. These techniques, based on Structure-from-Motion algorithms, offer the opportunity to study complex habitats or species with a strong three-dimensional component (Burns and Delparte, 2017), a case in point being the gorgonian forest where you can find the detailed population structure of *Paramuricea clavata* (Risso, 1826) and *Placogorgia* sp. (Palma et al., 2018; Prado et al., 2019a, 2019b). The use of a 3D approach is starting to become more widespread in studies of benthic sessile organisms, although they mostly focus on coral species and are less common with sponges (Prado et al., 2019a, 2021; Olinger et al., 2019). With this approach, important progress is being made in assessing coral reef rugosity (Leon et al., 2015; Young et al., 2018), or coral reef structural complexity (He et al., 2012; Ferrari et al., 2016). These parameters of structural complexity are related to the richness, epifauna abundance and an increase in the abundance of fish (Price et al., 2019).

In the framework of the project LIFE IP INTEMARES, and based on scientific knowledge, Spain is making great efforts to improve the management and consolidation of the Spanish Natura 2000 Network. "Banco de la Concepción" (hereafter BC), was declared a Site of Community Importance (SCIs) in 2014 and is located in the northeast of the

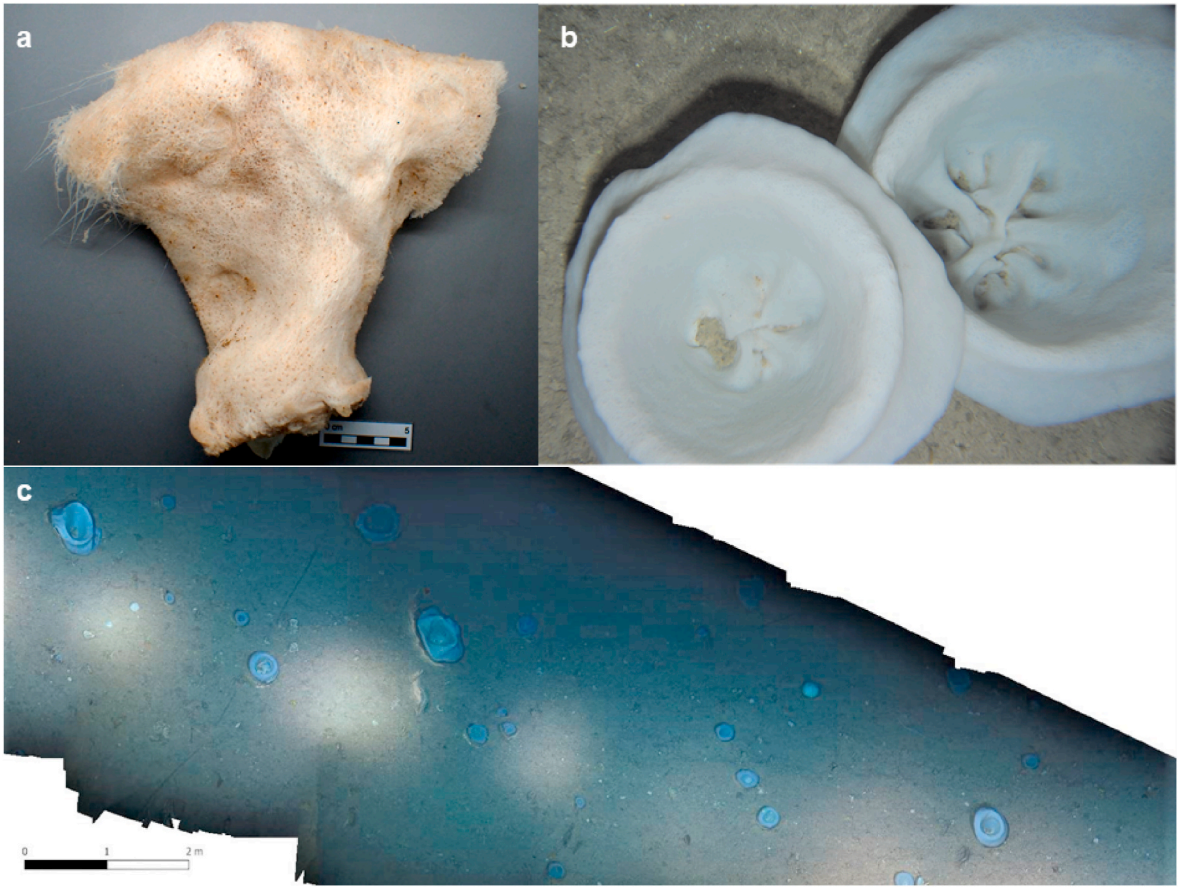

Fig. 1. Images of *Asconema setubalense* collected with dredges (a); observed with a Towed Vehicle (b) and an orthomosaic of several images of the video transect (c).

Canary Islands. Many species within the Reef Habitat 1170 of the Habitat Directive, have been documented in this area, including large hexactinellids, for instance the *Asconema setubalense*, or deep coral reefs of cold-water white corals such as *Desmophyllum pertusum* (Linnaeus, 1758), or *Madrepora oculata* Linnaeus, 1758. These species have a complex and three-dimensional structure that create habitats and represent sources of biodiversity (Davies et al., 2017; Prado et al., 2021). With the goal of enhancing knowledge in the area of biodiversity, and of mapping vulnerable habitats whilst causing the least possible damage to the environment, non-invasive methodologies were carried out in surveys within the BC. The vehicle used was a Remotely Operated Towed Vehicle (ROTV) named TASIFE. It carries a perpendicular-mounted full HD video-camera which provides a zenithal perspective, that with user-friendly software, facilitates the calibration and scaling of fine quality images of the seafloor.

Taking advantage of the characteristics of the images obtained with the TASIFE during a survey carried out at BC in 2018, the aims of the present study are: (a) to describe a functional methodology to measure specimens of *A. setubalense*, comparing 3D reconstruction techniques with photo analysis, called here a 2D approach; (b) to establish the most reliable measurement, with less variation between users, in order to define the size of the species using a 2D approach; (c) to present the height-size relationship of *A. setubalense* in BC; (d) to provide a population size structure of the species for the first time and (e) to establish a relationship between the size of *A. setubalense* and environmental variables. The results should be considered in future conservation directives, or in the development of indicators that show the good environmental state of habitats.

2. Material and methods

2.1. Study area

BC is an underwater mountain of volcanic origin located 75 km northeast of The Canary Islands. This seamount, together with the islands of Fuerteventura, Lanzarote and La Graciosa, is located in the eastern Canary Ridge (Fig. 2), which consists of a volcanic nucleus from the tertiary age, about 10 km thick, and covered by the product of subsequent eruptions (Guillou et al., 1996; Weigel et al., 1978; Van Den Bogaard, 2013). According to Spalding et al. (2007), this seamount is included in the ecoregion of the Azores, Canaries and Madeira (Lusitanian Province). BC represents the largest underwater mountain within The Canary Island Seamount Province, which comprises 16 main seamounts, the Canaries archipelago, and the Selvagens sub archipelago (Van Den Bogaard, 2013; Rivera et al., 2016). This seamount currently rises up to a height of 2433 m above the adjacent seafloor and has, as with other seamounts like Dacia or Essaouira, a completely or partly flat top, which in the case of BC has a diameter of around 45–50 km and a minimum depth of 158 m (Rivera et al., 2016). The steep flanks that bound it descend to depths ranging between 1700 and 2500 m and define a seamount base that is 66 km by 53 km (Rivera et al., 2016).

The study area is located between the subtropical gyre of the North Atlantic and the northwest African upwelling region. This means that the bank is influenced by The Canary Current, the presence of Taylor columns (a common process in seamounts in which the water uplifts, generating enclosed circulation cells and vertical mixing of water), and finally, filaments from the African coastal upwelling (Barton et al., 1998; IEO, 2013). These conditions make this area one of the most productive in the Canary Islands. The exposure to strong currents, depth range, and the high proportion of hard substrata compared to other deep-sea

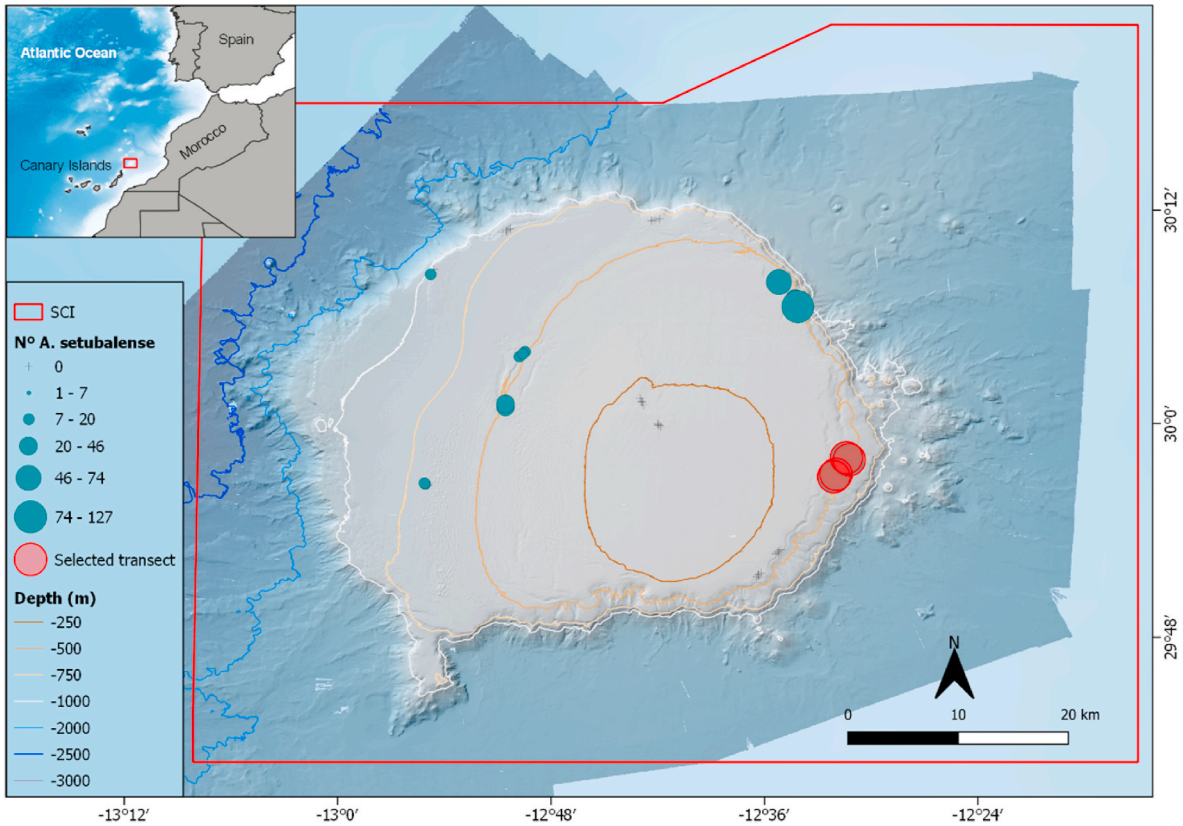

Fig. 2. Location of El Banco de La Concepción (upper left corner) and video transects of the survey INTEMARES-INTA4_CANARIAS_1118. Projected view (UTM Zone 28N, WGS84) with geographic coordinates (WGS84) indicated for reference. In red, the selected transects with the images of *Asconema setubalense* used for the analysis. The size symbol represents the abundance of *A. setubalense* in each transect.

ecosystems substrates, bring about a visibly dominant biota generally consisting of epibenthic coral and sponges. Fourteen main benthic assemblages have been described in BC, ten of which develop on different types of hard substrates, one of these assemblages is characterized by *Asconema setubalense* (IEO, 2013). This species was identified through samples collected at BC using dredges, and during surveys carried out in the previous project LIFE INDEMARES (IEO, 2013). All the specimens of this species were identified as *Asconema setubalense* (Tabachnick and Menshenina, 2007).

2.2. Data source

Within the LIFE INTEMARES project, the survey "INTEMARES-A4 CANARIAS 1118" was carried out at BC aboard the R/V Ángeles Alvariño in November 2018 with the aim of assessing the impact of fishing on habitat 1170 of The Habitat Directive (Council Directive 92/43/EEC on the Conservation of natural habitats and of wild fauna and flora). In total, 56 transects, covering about 9 km, and with 19 h of video recording, were performed in the study area using the ROTV TASIFE (Fig. 3). This vehicle, which can operate up to a depth of 2000 m, is a perpendicular-mounted High-Definition camera (Nikon D800 AF Nikkor 20mm/f2.8D) equipped with two light sources (LED DSPL Sphere SLS-5000), and two parallel green SeaLaser 100s (532 nm), with a distance of 10 cm between them for scaling and measuring images. On board the TASIFE, an acoustic underwater positioning and navigation system (HiPAP 500), provided the location, velocity and heading of the vehicle. The Zenithal perspective was used to obtain calibrated high resolution and fine quality images of the seafloor. In particular, this position favours accurate measurements of the size of some species such as the sponge *Asconema setubalense*.

Within the study area a total of 1110 specimens of *A. setubalense* were identified in 30 out of the 56 transects, each of them with an exact duration of 20 min and found between depths of 165 m and 1350 m. To carry out a comparative analysis of the measurement methodology, 40 specimens of *A. setubalense* were selected and measured. Specimens with different sizes were chosen, covering the range of sizes observed in the transects. They were chosen from four different video transects, on the west side of the bank, where the highest density of *A. setubalense* can be found (Fig. 2). These sections, that covered a total area of 1701 m^2, were on hard substrate, between a depth of 385 and 420 m, and with low slopes filled with sediment.

2.3. Image analysis

The different measurements obtained from the *A. setubalense* specimens, diameter, perimeter and surface area, were calculated using two different software ImageJ (version 1.52a; Schneider et al., 2012) for 2D analysis, and Pix4D Mapper Pro software (Pix4D SA, Switzerland) for 3D analysis. With ImageJ, different 2D measuring tools were used and compared: lines to measure the diameter and polygon selection, and a wand tool for the surface area. With the aim of assessing which measurement and methodology is the most stable and reliable for a 2D approach, all the 2D measurements were calculated by 3 different users (Fig. 4). This test was not carried out with different users in the 3D approach since this method is assumed to have a higher reliability factor, due to the advanced automatic triangulation of the 3D software.

For the 2D image approach a VLC media player (open source; VideoLan, 2006) was used to collect the images or frames of the video sections where the sponge is whole and in the centre of the image. These images were measured by three different users that collected data on the diameter, the surface area, and the perimeter of the funnel using the ImageJ software, whilst taking into consideration the distance between laser beams when scaling the images. This software is an open-source Java-written program that carries out a range of image-analysis methods and approaches that are easily accessible to the scientific community. After scaling the images, a line segment tool was used to take four measurements of the diameter (Fig. 4); a mean value was used for the subsequent analysis. Surface area and perimeter measurements were taken using two different methods: a polygon tool, which, by clicking repeatedly the mouse, creates irregularly shaped selections defined by a series of line segments, and the automatic outlining tool, or wand tool, which traces the edge of the object, after setting a colour threshold for the image (Fig. 4).

In the 3D analysis, video-sections were decomposed into thousands of geo-positioned overlapping images using photogrammetric Pix4D Mapper Pro software. This software carries out an advanced automatic triangulation based purely on image content and an optimization technique (Tola et al., 2010). The triangulation algorithm is based on binary local key points, that search for matching points by analysing all the images. Those matching points, as well as the approximate values of image positions and orientation provided by the HiPAP system on board the TASIFE, are used in a bundle adjustment to reconstruct the exact position and orientation of the camera for every acquired image. Focal

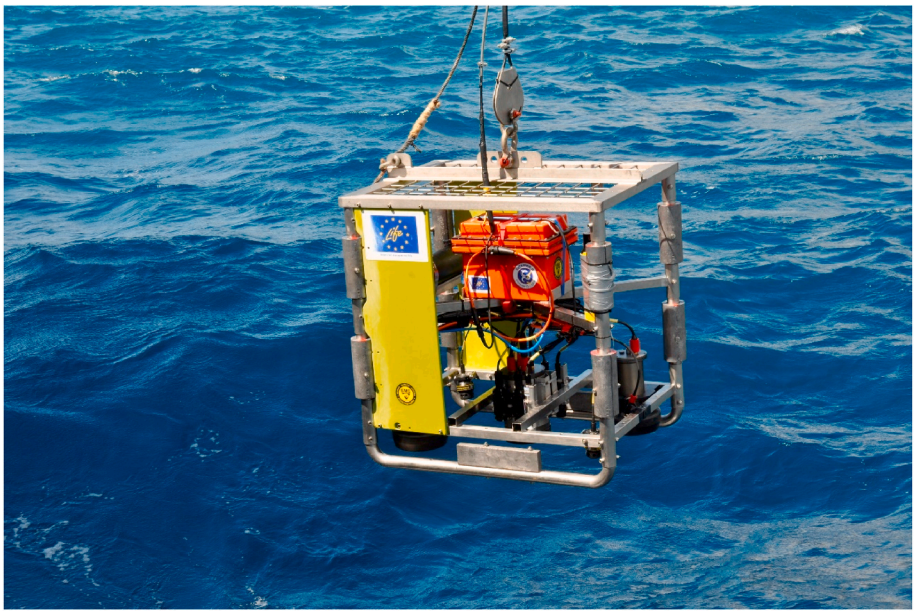

Fig. 3. The ROTV TASIFE, with an approximate size of 1m in length, width and height.

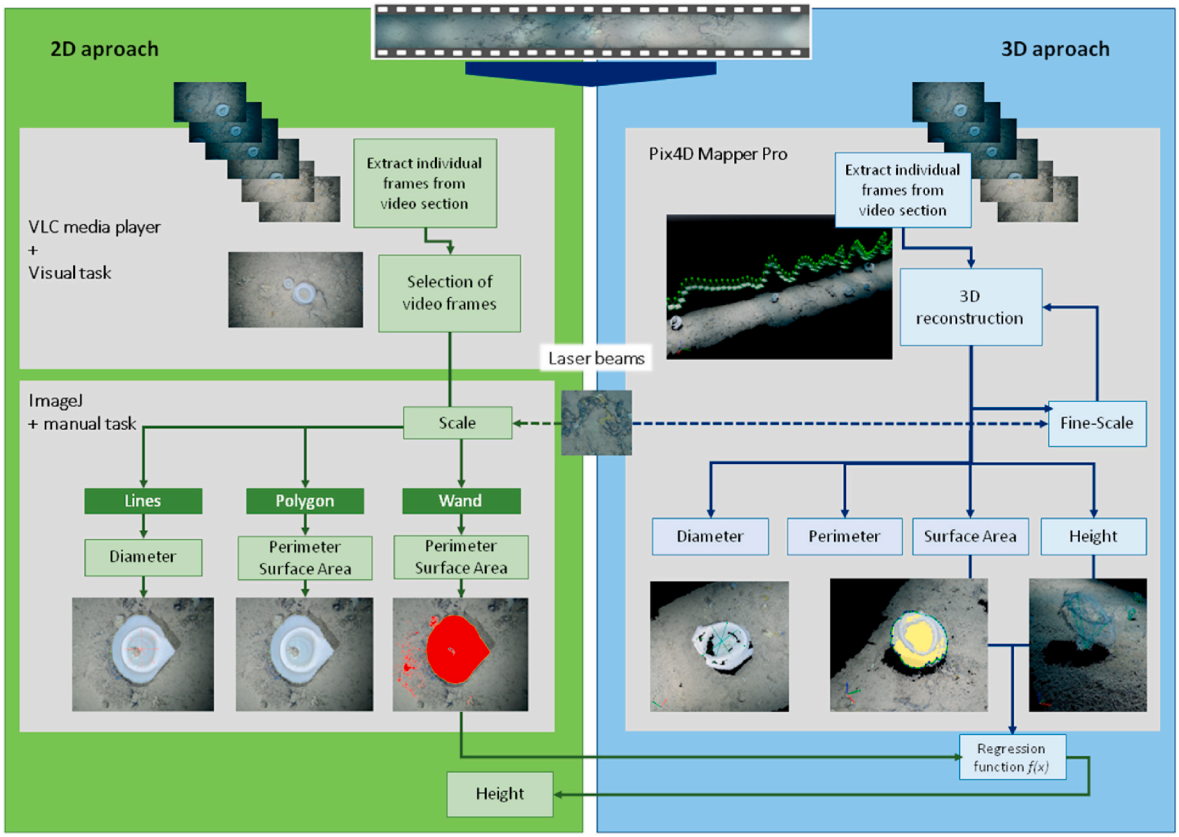

Fig. 4. Diagram of the methodology applied in this study with the steps carried out in 2D and 3D approaches in order to obtain each measurement.

length, principal point and radial/tangential distortions of the camera were set as initial theoretical values, while the final internal and external orientation parameters were determined by bundle adjustment processing. The distance between parallel laser beams (10 cm apart) is used as a reference scale. Several scale constraints are used to fine-scale and optimize the 3D reconstruction. With the completed automated integration of tie point measurements, camera calibration, and positional data given by the cameras and scale constraints, the software provides 3D dense point clouds, orthomosaics and digital surface models (DSM). Since all the information is geo-referenced by a cartographic system (UTM-WGS84), all the obtained geographic layers can be included in a GIS. Diameter, maximum cup-surface area, external perimeter, and height of the *A. setubalense* sponges were measured in a 3D point cloud with Pix4D tools. Due to the irregular form of the sponge, it was necessary to take several measurements of all the morphometric parameters, and to consider the mean values (Fig. 4).

2.4. Data analysis

Values for the three morphometric variables obtained with the different tools and software were calculated, in the case of 2D, by three different users. After a descriptive analysis, a Shapiro-Wilks test was applied to evaluate the normality of the morphometric data and the distance between lasers (in this case the number of pixels between lasers that correspond to the known distance of 10 cm), and the result was significant for all data ($p < 0.001$).

To carry out a comparative analysis of the 2D measurements of the different users, log transformation was performed on the data. This was carried out in order to obtain a normal distribution, and to be able to carry out an ANOVA test, as well as testing the sphericity of the data using Mauchly's sphericity test. This analysis was carried out with the package *ez* (Lawrence, 2016) of the R program (R Core Team, 2020). Subsequently, the 2D and 3D measurements were compared to detect similarities between the two approaches, using the paired Wilcoxon Signed-Rank Test, with the help of Scatter plots.

A linear regression was applied to examine the correlation between the surface area, taken with a 2D wand tool, and the height, that was measured with a 3D technique, in order to evaluate any possible relationship between these variables. Additionally, a quadratic regression was also calculated in order to show more clearly the graphic distribution of the data, and the available knowledge on the growth of the species. An ANOVA analysis was used to test which regression is better at describing the data, although, the selection of the best regression also depends on which one reflects better the behaviour of the dependent parameter (height), when there is a change in the explanatory variable (surface area). For this analysis the R packages *ggplot2* (Wickham, 2016), *hrbrthemes* (Rudis, 2020) and *ggpubr* (Kassambara, 2020) were used.

Following the results of the comparative analysis between methods, the sizes of all the specimens observed in the study area were measured with the selected 2D approach. In addition, the regression that most accurately represented the surface area-height relationship of the species was used to calculate the height of all the specimens. These measurements were used to represent the size frequency distribution of *A. setubalense* for the BC.

The relationship between the size (surface area) of *A. setubalense* and environmental variables, and geomorphologic data, was explored using Generalized Additive Models (GAM). A GAM is a non-parametric, regression technique not restricted by linear relationships, and is flexible regarding the statistical distribution of the data. GAMs have been widely applied to investigate relationships between environmental factors and data on the presence, or abundance of species (Pajuelo et al., 2016). They are mainly used to predict spatial distribution (Guisan and Zimmermann, 2000; Serrano et al., 2017a; Ramiro-Sánchez et al., 2019), however GAMs have not been used to analyse the distribution of the sizes of a species. In this case, a model was built assuming a Gaussian distribution of errors, with an identity link function and smoothing

splines to explore the relationship between the size of *A. setubalense* and the following variables: depth, aspect (measured by indices of eastness and northness), reflectance, slope and roughness. These data were acquired using an echosounder during the INDEMARES (IEO, 2013) and INTEMARES surveys that were carried out within the study area, obtaining layers with a final resolution of 20 m. Correlation between variables was examined using Spearman's correlation coefficient. Roughness had a high correlation with slope and depth (correlation values > 0.7), so it was removed from the analysis. This GAM-based analysis used the *mgcv* package (Wood, 2017), and deviance explained, adjusted r2, and GCV scores were calculated. The shapes of the selected variables were plotted and a predictive map of sponge sizes was represented. Other variables such as the velocity of currents, or other oceanographic parameters, important in the distribution of other deep-sea sponges (Bell et al., 2017; Kazanidis et al., 2019; Ramiro-Sánchez et al., 2019) were not available for the present study.

3. Results

Data for the 40 specimens measured by 2D and 3D approaches show a high abundance of small specimens and a strong asymmetry (Table 1). For instance, they show in the 2D-polygon a median surface area of 0.068 m^2, although the maximum value that was measured was 1.02 m^2 and the minimum 0.003 m^2 (Table 1).

3.1. Comparison between 2D users, methods, and morphometric measurements

The distance between lasers showed a difference between users of 0.465 ± 0.239 pixels, within a range of 0.0–2.74 pixels. The Two-way repeated measures ANOVA found no significant differences to distort the previous analysis.

For each parameter (Table 1), the measurements present a similar distribution of data among users and methods. Two-way repeated measures ANOVA found a statistically significant difference between users for diameter (Table 2). In the case of the perimeter, significant differences were found for the two factors (user and method), as well as for the interaction user-method. On the contrary, the measurements for the surface area were not significantly different between users, methods, or interaction (Table 2). Mauchly's Sphericity test was statistically significant for perimeter (User: W = 0.423, p = 0.000; Method: W = 0.344, p = 0.000) and surface area (User: W = 0.571, p = 0.000; Method: W = 0.507, p = 0.000), so the alternative hypothesis that the variances of the differences are not equal was accepted. Consequently, a Greenhouse-Geisser correction to the degrees of freedom was applied and an adjusted p-value was obtained (Table 2). These results suggest that the surface area is the morphometric measurement that presents the least variation between different methods and users.

Table 2
Two-way repeated measures ANOVA of the log transformed variables of diameter, perimeter, and surface area of the 40 *Asconema setubalense* specimens with the user factor (3 levels) and method factor (2 levels, only for perimeter and surface area). (G) Degrees of freedom and adjusted *p*-value modified by Greenhouse-Geisser correction.

	df	sum sq	mean sq	f value	pr(>f)
Diameter					
User	2	0.0691	0.0345	10.64	0.001
Perimeter					
User	$1.3^{(G)}$	0.0496	0.0248	7.578	$0.005^{(G)}$
Method	1	0.5084	0.5084	209.4	0.000
User*Method	$1.2^{(G)}$	0.0724	0.0362	14.67	$0.000^{(G)}$
Area					
User	$1.4^{(G)}$	0.0036	0.0018	0.933	$0.369^{(G)}$
Method	1	0.0045	0.0045	3.306	0.077
User*Method	$1.3^{(G)}$	0.0040	0.0020	2.378	$0.12^{(G)}$

Pairwise comparisons for diameter and perimeter, using a pairwise paired *t*-test with a Bonferroni adjustment, show that the diameter measurements of user 3 were significantly different from the other users (Table 3). In the case of perimeter measurements, significant differences were found between users applying the same methods, but not between user 3 and user 2 with the polygon tool, or users 2 and 1 with the wand tool. Comparisons between methods for each user gave a significantly different result for all cases (Table 3).

3.2. Comparison between 2D-3D techniques

Scatter plots (Fig. 5) represent the relationship between the 2D and 3D measurements for all parameters. It shows 2D measurements of diameter are higher than 3D values for the same specimens. Differences are also observed for perimeter data between 3D and 2D, as well as for polygon and wand tools. In the case of variable surface area, the data for the two techniques are similar for most of the specimens with a difference of less than 0.25 m^2, but specimens of a larger size have measurements with higher differences (Fig. 5c), these differences being both positive and negative. The Wilcoxon Signed-Rank Test verified these results and showed significant differences between diameter and perimeter measurements obtained with a 3D approach, and the mean values obtained using 2D techniques (Diameter: V = 684, p-value = 0.0001; Perimeter: V = 193, p-value = 0.0029), but not for surface area (V = 434, p-value = 0.7547).

Table 1
Summary data for all measurements, techniques and methods applied in the morphometric analysis of the 40 measured specimens of *A. setubalense*.

Morphometric measurement	Method	User	mean	SD	min	Q1	median	Q3	max
Diameter (m)	3D	3D	0.276	0.188	0.05	0.119	0.215	0.361	0.717
	Polygon	User1	0.303	0.219	0.055	0.123	0.216	0.429	0.772
		User2	0.298	0.22	0.052	0.119	0.208	0.428	0.783
		User3	0.312	0.22	0.051	0.129	0.236	0.434	0.805
Perimeter (m)	3D	3D	1.493	1.17	0.209	0.517	0.978	2.111	4.121
	Polygon	User1	1.392	1.067	0.201	0.531	0.94	2.026	3.838
		User2	1.373	1.042	0.197	0.522	0.939	2.02	3.604
		User3	1.367	1.033	0.202	0.531	0.928	1.991	3.608
	Wand	User1	1.491	1.142	0.216	0.568	1.009	2.118	4.066
		User2	1.46	1.099	0.216	0.562	1.002	2.128	3.817
		User3	1.571	1.181	0.22	0.593	1.095	2.218	4.131
Area (m^2)	3D	3D	0.214	0.275	0.003	0.019	0.066	0.295	0.924
	Polygon	User1	0.214	0.283	0.003	0.021	0.069	0.279	1.027
		User2	0.212	0.282	0.003	0.021	0.068	0.28	1.001
		User3	0.211	0.279	0.003	0.021	0.068	0.279	1.003
	Wand	User1	0.212	0.281	0.003	0.021	0.069	0.278	1.02
		User2	0.214	0.283	0.003	0.021	0.069	0.283	1.012
		User3	0.21	0.277	0.003	0.02	0.068	0.276	0.991
Height (m)	3D	3D	0.437	0.248	0.112	0.217	0.364	0.67	1.038

Table 3
Pairwise comparison for the diameter (between users) and perimeter variables (between users and methods).

	group1	group2	statistic	df	p	p.adj	signif.
Diameter							
	User3	User2	4.38	39	8.74e-5	2.62e-4	***
	User3	User1	2.61	39	1.30e-2	3.80e-2	*
	User2	User1	−2.04	39	4.80e-2	1.45e-1	ns
Perimeter by Method							
Polygon	User3	User2	−0.636	39	5.28e-1	1	ns
	User3	User1	−2.68	39	1.10e-2	0.032	*
	User2	User1	−2.98	39	5.00e-3	0.015	*
Wand	User3	User2	3.86	39	4.13e-4	0.001	**
	User3	User1	2.97	39	5.00e-3	0.015	*
	User2	User1	−1.50	39	1.41e-1	0.423	ns
Perimeter by User							
User3	Polygon	Wand	−7.96	39	1.07e-9	1.07e-9	****
User2	Polygon	Wand	−16.3	39	5.55e-19	5.55e-19	****
User1	Polygon	Wand	−11.2	39	1.02e-13	1.02e-13	****

3.3. Relationship between the surface area and height of the specimens

The lineal regression between height, and 2D surface area measurements taken with the wand tool, showed a significant and positive relationship ($R^2 = 0.69$, $p < 0.001$) (Fig. 6). This relationship is more evident in small sponges of less than 0.4 m^2, than in large specimens with irregular forms. Quadratic regression also showed a significant relationship and a better data adjustment ($R^2 = 0.81$, $p < 0.001$). ANOVA analysis between linear and quadratic models concluded that the quadratic model is significantly better when describing the relationship between these morphometric variables ($F = 18.465$, $p < 0.001$). Both regressions present a minimum height value, produced by the regression constant, which is 0.2 in the quadratic, and 0.27 in the lineal regression. As a consequence, very small sponges (<0.06 m^2), assume higher height values. This occurs because these small specimens that were used for regressions presented a relatively wide range of heights (0.1–0.26 m), with a mean of 0.19 m. Only four individuals with a surface area of less than 0.01 m^2, had a height value of less than 0.2 m.

3.4. Population size structure of A. setubalense

The surface area (m^2) of a total of 1035 specimens of *A. setubalense* in BC was measured with a 2D wand tool and 75 specimens were discarded, for among other things, not fitting entirely within the image frame, or for having been damaged. Fig. 7A shows the unimodal surface area frequency distribution of the *A. setubalense* and a strong asymmetry with a positive skew: specimens show a median of 0.10 m^2, with the most abundant size-class being 0–0.1 m^2, although the maximum value measured is 2.76 m^2 (Fig. 7A). The histogram of heights (Fig. 7B) has a similar distribution, with a high frequency for the smaller sizes, smaller than 0.25 m, but more similar frequencies up to the maximum size-class of 0.85 m.

3.5. Relationship between the surface area and environmental variables

The resulting GAM model presents an adjusted $R^2 = 0.139$, a deviance explained = 15.4%, and a minimised generalized cross-validation (GCV) = 0.118. The model shows a significant relationship between all the parameters (Table 4). The model suggests that the size of *A. setubalense* increases slightly and monotonically with northness and eastness. Furthermore, the size has maximum values at a depth of between 400 and 500 m. The relationship with reflectance reaching maximum levels at values of −20 and −25 (mixed substrata). Similarly, bottoms with a slope of 5° seem to be more appropriate for bigger sponges (Fig. 8). A predictive map (Fig. 9) of the model locates areas with large specimens in a band crossing the flat top between a depth of 400 and 500 m, and in the bank's shelf with mixed substrata, and with a depth of between 800 and 1000 m.

4. Discussion

4.1. Advantages and disadvantages of each technique and measurement

In the present case, 3D reconstruction techniques with orthomosaics

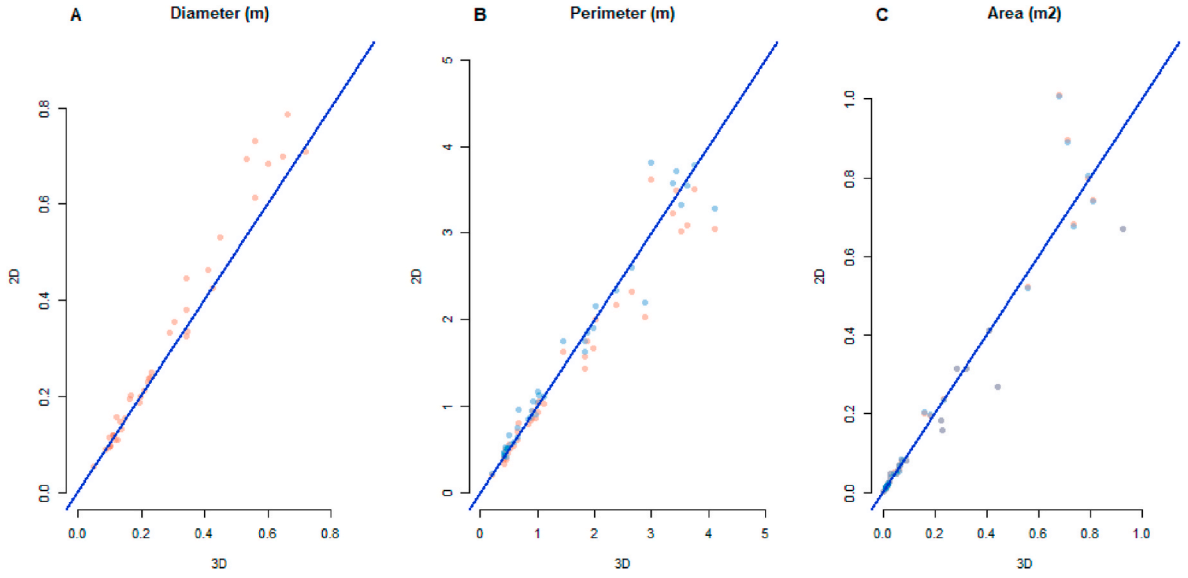

Fig. 5. Scatter plot for diameter, perimeter, and surface area measurements with 2D and 3D techniques. Blue points: measurements with "wand tool"; red points: measurements with "line or polygon selection tool". Points that fall above the blue line indicate cases for which the value for 2D was greater than that of 3D.

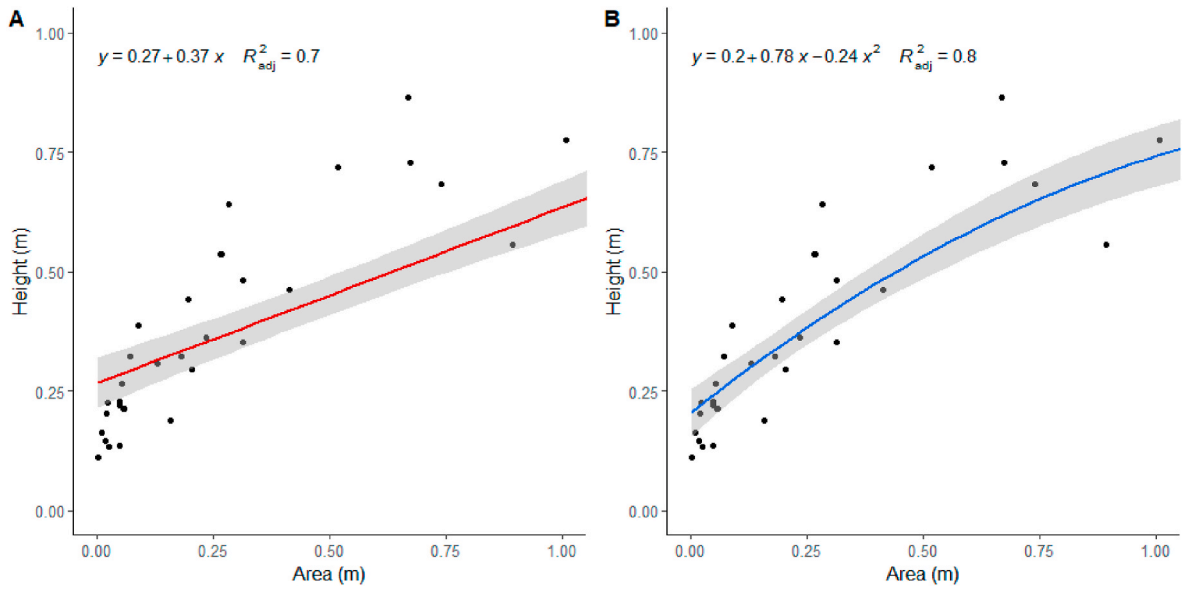

Fig. 6. Relationship between the surface area, measured with a wand tool using a 2D technique, and height, measured with a 3D technique, of the specimens of *A. setubalense.* A) Lineal and B) quadratic regression.

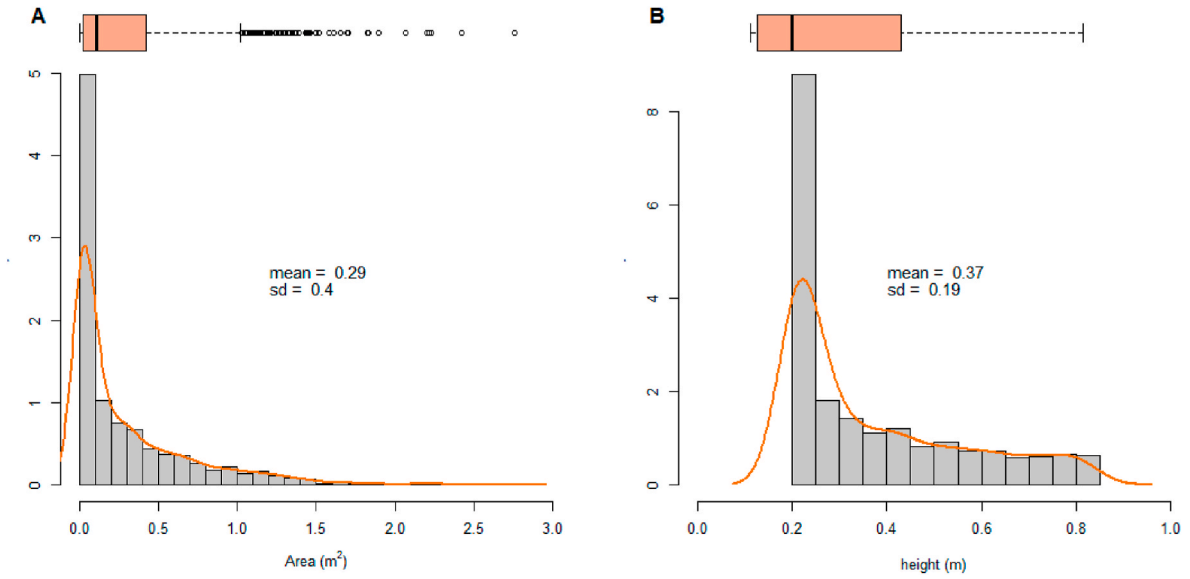

Fig. 7. Histogram and boxplot of the surface area measured with a 2D wand tool (A) and height obtained from the quadratic regression (B) of the 1035 specimens of *Asconema setubalense* sampled in BC.

Table 4
Results of the Gaussian GAM for the surface area of *A. setubalense* and the geomorphologic parameters.

Variables	edf/df	F	p-value
Eastness	1	4.707	0.031
Depth	5.74	7.377	0.000
Northness	1	7.526	0.023
Reflectance	6.07	2.677	0.002
Slope	4.43	8.262	0.003

of the images have provided complete images of the sampled area, giving an estimation of the height of the sponges, something the 2D approach did not allow for in its measurements. With other benthic species it is possible to measure other important parameters, such as the orientation of the specimens or colonies (Prado et al., 2019b, 2021). However, these techniques require the use of complex programs, a prior preparation of the images to carry out a complete 3D reconstruction, and a time-consuming, and intensive training process for technical staff to be able to manipulate the software. Thus, other simpler alternatives can make morphometric data more accessible in biological and ecological studies in diverse fields, such as taxonomy, or in the description and conservation of habitats. This was the case with the 2D approach described here, which is a widely known technique that has been applied in similar studies (Bo et al., 2015; Prouty et al., 2011; Palma et al., 2018), The 2D technique described in this study, using zenithal images with a high resolution and a 2D approach, has been very useful in the case of *Asconema setubalense*. It can also be used to study other benthic species (Fig. 10), especially those where images facilitate taxonomic identification, and where morphology is more easily measured using top-down images, as is the case with some sponges and echinoderms. This method could also be used to estimate the cover of

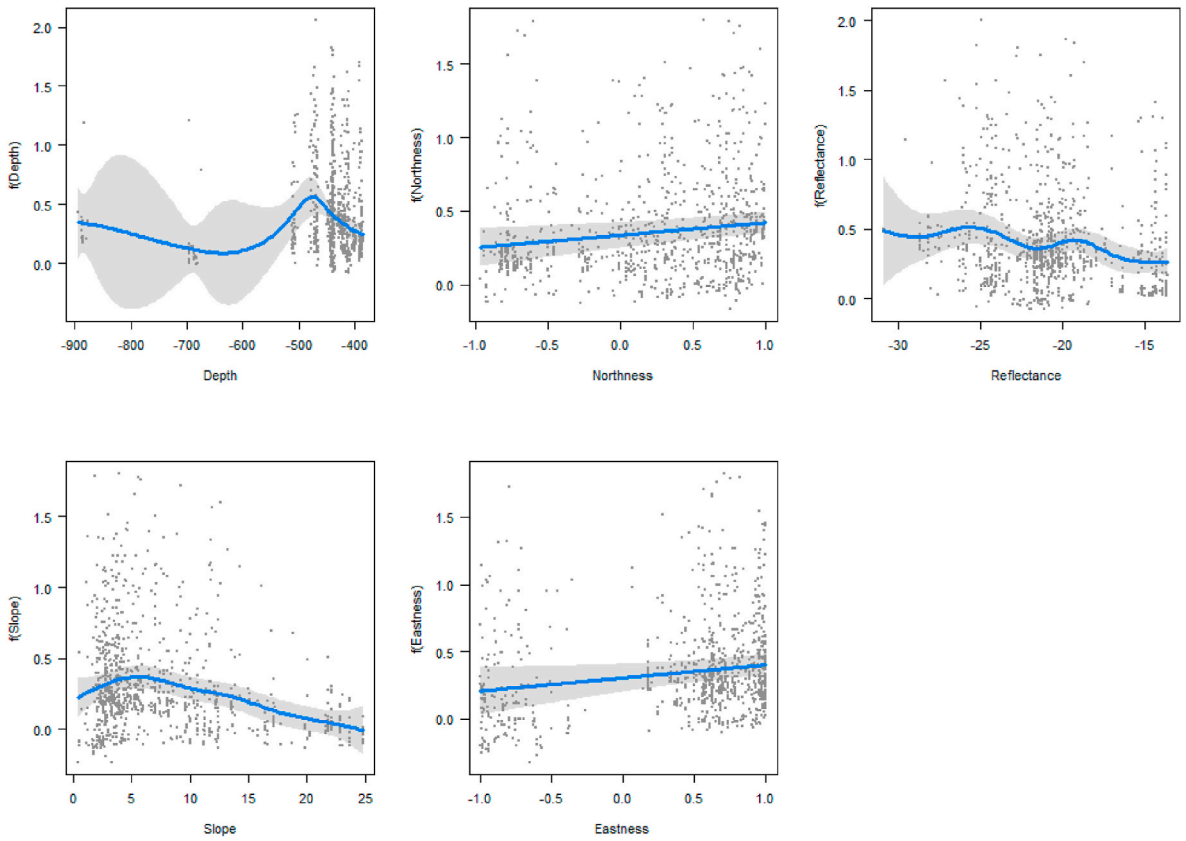

Fig. 8. Effect of each variable in the GAM model for the size of *A. setubalense* and the geomorphologic parameters. The shaded grey area corresponds to a 95% confidence interval and the points are partial residuals.

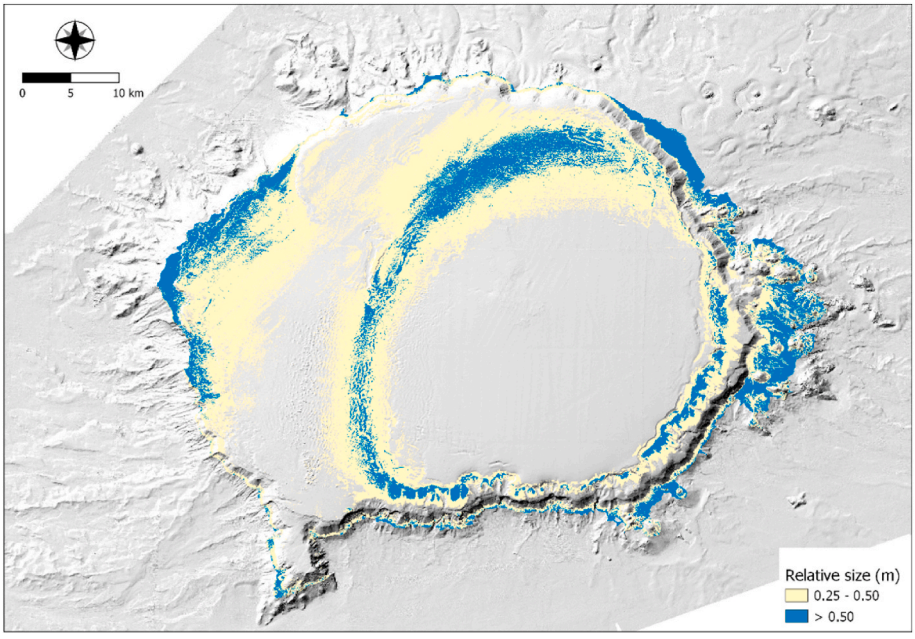

Fig. 9. Map of the relative size of *A. setubalense* in BC. The areas coloured yellow and blue show areas where there is a high probability of finding large sizes of this sponge. The Model was limited to depths of up to 1300 m, representing only the bathymetry range covered in this study.

framework-building cold-water corals, such as *Desmophyllum pertusum*, *Solenosmilia variabilis* Duncan, 1873, or *Madrepora oculata*, species considered to be some of the most important ecosystem engineers of the seafloor (Freiwald, 2011). Nevertheless, a 3D approach is currently the most appropriate method to get more complete and precise data of species with a complex three-dimensional form.

One of the main conclusions of this study is that the selection of the appropriate morphological parameters to analyse and describe the species could be crucial in obtaining reliable results (Mistri, 1995). In most of the related studies, diameter is the selected parameter used to

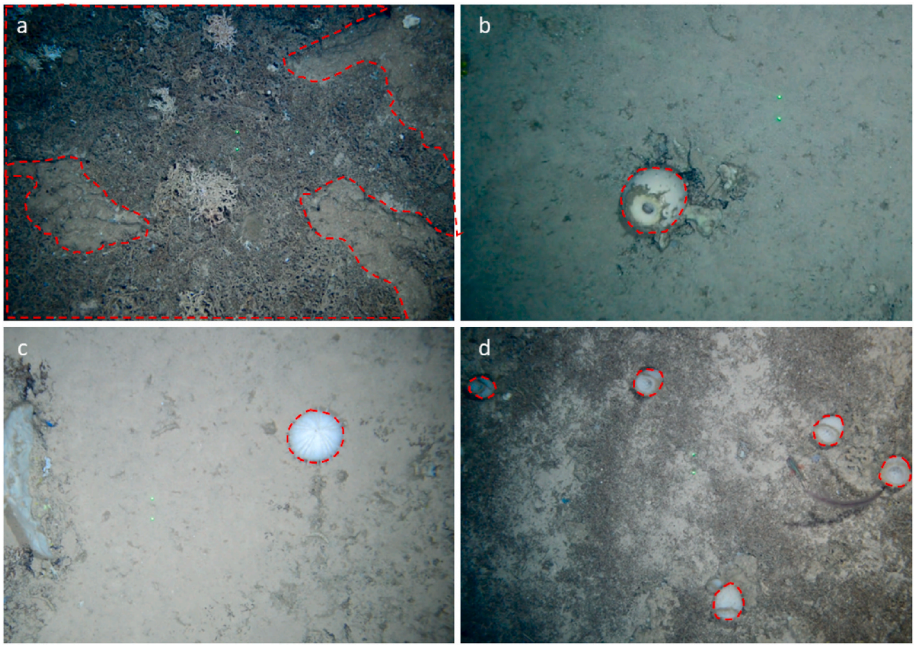

Fig. 10. Some examples of benthic species in which the methodology used in the 2D approach described in this study can be applied. a) *Madrepora oculata*; b) sponge *Geodia* sp.; c) sea-urchin *Echinus melo*; d) sponge *Pheronema carpenteri*.

describe the size of these hexactinellids (Barthel et al., 1996; Tabachnick and Menshenina, 2007; Prado et al., 2021; Sánchez et al., 2009). This measurement is taken from the highest part of the specimen's cup (Prado et al., 2021), and normally the average of at least four crossed diameters are necessary to get a representative value, especially when the sponge has an irregular form. To measure this parameter, the user has to select the initial and end measurement points, and these decisions are probably responsible for the high deviance of data, and significant differences between users in this measurement. Something similar occurs with perimeter, thus it could be difficult to distinguish the limits of the sponge in some images. On the contrary, after setting the image's colour threshold, the wand tool is automatic, tracing the edge of the sponge, which allows fewer steps in the measurement process and less deviance. Therefore, it should be used in future studies on the size of the species, instead of the diameter. These variabilities caused by the users should always be taken into account in future studies with other techniques, parameters or species (Ninio et al., 2003).

4.2. Relationship between the surface area and height of A. setubalense

Regarding the relationship between size and height, Tabachnick (2002) previously stated that the maximum diameter of specimens is usually similar to the length. In general, references that include data on the size of this sponge, indicate descriptively the size and height of specimens without providing any function which could be used to model the relationship between them (Tabachnick, 2002; Sánchez et al., 2009; Prado et al., 2021). Considering this, the present study provides two significant functions to explain the relationship between surface area and height: linear and quadratic. The linear model shows a positive, and almost proportional increase between height and surface area, and is more evident in small sponges. However, this relationship does not seem to happen with large specimens. When this species reaches a maximum size, its shape seems to become irregular, growing more in extension than in height. Moreover, and despite the fact that this species is known for its large size, its growth is not unlimited; the holotype is about 600 mm in length (Tabachnick and Menshenina, 2007), and the maximum size that has been registered has a diameter and height of about 1m (Prado et al., 2021). Therefore, the obtained quadratic function is more appropriate than the linear one when observing the growth of these species. Small specimens with a funnel-like body show a clear area-height relationship, but bigger ones, where the marginal parts start to evert and turn downwards, and where the osculum has an irregular form, do not share this proportional area-height relationship (Prado et al., 2021). This kind of relationship between size parameters has also been observed in other hexactinellid sponges. Leys and Lauzon (1998) describe how the relationship between estimators of size for the sponge *Rhabdocalyptus dawsoni* (Lambe, 1893) also changes depending on the size. An aspect to be considered is that both regressions apparently show a flaw, being more accused in the lineal one, and caused by the regression constant, giving very small sponges a relatively higher height. Therefore, this relationship should be used with care in these very small sponge sizes, and should be analysed in depth in future studies.

4.3. Size structure and distribution

The location and distribution of *A. setubalense* are important given the vulnerability and the level of threat to these habitats (OSPAR, 2008). Most studies show information on the distribution, maximum size, density (Tabachnick and Menshenina, 2007; Sánchez et al., 2009, 2017; De la Torriente et al., 2018; Prado et al., 2021), or even the medium size of adult specimens (OSPAR, 2010). The Present study goes a step further and presents the first description of the size structure of *A. setubalense,* with such a large volume of data, that it is not possible to compare it with other databases and other regions. The size structure obtained for the populations shows a high abundance of small specimens with a surface area of less than 0.1 m^2, with just a few large individuals with a surface area of 0.6–0.8 m^2 occupying, in some instances, almost the entire frame of the video images. Other studies with other species of sponges also describe unimodal size-frequency distributions with a lesser number of large specimens (Bo et al., 2012; Kazanidis et al., 2019; Santín et al., 2019). The high abundance of small specimens, considered as juveniles (OSPAR, 2010), could be related to incidences of pulse recruitment (Santín et al., 2019), or intense fishing activity (IEO, 2013). Some authors suggest that a particular organic carbon flux may influence recruitment or regeneration in hexactinellid deep-sea sponges (Kahn et al., 2012). In any case, it will be necessary to monitor the conservation status of the populations of this species over time in BC, aided by the contribution of the present study.

The GAM model was applied to detect patterns of size distribution of *A. setubalense* which were not initially evident. The model shows a significant relationship with geomorphologic parameters, mainly depth, showing that larger specimens tend to be found in two depth ranges: one between 400 and 500 m, and another in deeper bottoms of around 800m. This distribution seems to be similar to other deep species such as *Pheronema carpenter* (Thomson, 1869), where small individuals appear only in the upper distribution zone of the species (Barthel et al., 1996). The map of the size distribution of *A. setubalense* in BC should be looked at with caution and not be confused with the species' distribution areas. Certainly, it provides areas where the specimens of this species are larger, and therefore these areas should be taken into consideration in future management plans for the SCI. Prior to this step, and with the aim of getting a better model for size distribution, it is necessary to consider other parameters in the model, such as oceanographic, anthropogenic and even biological variables. These were not available for the present study, but that have been recognised as important in other studies, (Bell et al., 2017; Kazanidis et al., 2019; Ramiro-Sánchez et al., 2019).

The characterization of *A. setubalense* populations has a special relevance for conservation and management measures in the Banco de la Concepción. Currently, fishing activity, which was previously more intensive, is the only relevant pressure identified in this area, and is currently represented by the longline fishery (IEO, 2013). Another future step is to analyse the possible effects of the longline fishing activity that takes place in the bank, especially on larger sponge specimens. The present study can be applied in the framework of the Marine Strategy Framework Directive, the Habitats Directive, and the FAO Vulnerable Marine Ecosystems (VME) regulations.

5. Conclusions

It is obvious that images not only offer a qualitative description of species or habitats, but also provide essential quantitative data on parameters such as abundance, density, or size, factors that can be used to establish the conservation status of hard-to-access species or ecosystems. These parameters are important to monitor the conservation status of populations of species or communities.

The results of this study enhance the knowledge of this species, whilst the methodology carried out on the A. *setubalense* can be applied to other regions, or even to the other species of the genus *Asconema* that are distributed throughout the Atlantic Ocean. Comparative studies of their populations and their size structure can shed light on the conservation status of the global populations, interspecific relationships, and the influence of different environmental parameters, or anthropogenic impacts on the population structure.

Declaration of competing interest

The authors declare that they have no known competing financial interests or personal relationships that could have appeared to influence the work reported in this paper.

Acknowledgements

The authors would like to thank all the participants and crew of the R/V Ángeles Alvariño for their collaboration in achieving the objectives during the INTEMARES-INTA4_CANARIAS_1118 survey. Thanks to the geomorphologic description and characterization of the BC, carried out by Natalia Martínez-Carreño and colleagues from the Oceanographic Center of Málaga (CSIC-IEO), it was possible to carry out the GAM model. We are also grateful to Jose Manuel González Irusta for the revision of the GAM model and Younn Brizard for helping us in the selection of some images for the article.

This research has been carried out in the scope of the LIFE IP INTEMARES project, coordinated by the Biodiversity Foundation of the Ministry for the Ecological Transition and the Demographic Challenge. It receives financial support from the European Union's LIFE program (LIFE15 IPE ES 012).

References

Barthel, D., Tendal, O.S., Thiel, H., 1996. A wandering population of the Hexactinellid sponge Pheronema carpenteri on the continental slope off Morocco, northwest Africa. Mar. Ecol. 17, 603–616. https://doi.org/10.1111/J.1439-0485.1996.TB00420.X.

Barton, E.D., Aristegui, J., Tett, P., Canton, M., García-Braun, J., Hernández-León, S., Nykjaer, L., Almeida, C., Almunia, J., Ballesteros, S., Basterretxea, G., Escanez, J., García-Weill, L., Hernández-Guerra, A., López-Laatzen, F., Molina, R., Montero, M. F., Navarro-Peréz, E., Rodríguez, J.M., Van Lenning, K., Vélez, H., Wild, K., 1998. The transition zone of the Canary Current upwelling region. Prog. Oceanogr. https://doi.org/10.1016/S0079-6611(98)00023-8.

Beazley, L.I., Kenchington, E.L., Murillo, F.J., Sacau, M.D.M., 2013. Deep-sea sponge grounds enhance diversity and abundance of epibenthic megafauna in the Northwest Atlantic. ICES J. Mar. Sci. https://doi.org/10.1093/icesjms/fst124.

Bell, J.J., Biggerstaff, A., Bates, T., Bennett, H., Marlow, J., McGrath, E., Shaffer, M., 2017. Sponge monitoring: moving beyond diversity and abundance measures. Ecol. Indicat. 78, 470–488. https://doi.org/10.1016/J.ECOLIND.2017.03.001.

Bo, M., Bavestrello, G., Angiolillo, M., Calcagnile, L., Canese, S., Cannas, R., Cau, Alessandro, D'Elia, M., D'Oriano, F., Follesa, M.C., Quarta, G., Cau, Angelo, 2015. Persistence of pristine deep-sea coral gardens in the Mediterranean Sea (SW Sardinia). PLoS One 10, 1–21. https://doi.org/10.1371/journal.pone.0119393.

Bo, Marzia, Bertolino, M., Bavestrello, G., Canese, Simonepietro, Giusti, M., Angiolillo, M., Pansini, M., Taviani, Marco, Bo, M., Bertolino, Á.M., Bavestrello, Á. G., Canese, S., Giusti, Á.M., Angiolillo, Á.M., Taviani, M., 2012. Role of deep sponge grounds in the Mediterranean Sea: a case study in southern Italy. Hydrobiol. (Sofia) 6871 687, 163–177. https://doi.org/10.1007/S10750-011-0964-1, 2011.

Burns, J.H.R.R., Delparte, D., 2017. Comparison of commercial structure-from-motion photogrammetry software used for underwater three-dimensional modeling of coral reef environments. In: The International Archives of the Photogrammetry, Remote Sensing and Spatial Information Sciences. International Society for Photogrammetry and Remote Sensing, pp. 127–131. https://doi.org/10.5194/isprs-archives-XLII-2-W3-127-2017.

Cuvelier, D., de Busserolles, F., Lavaud, R., Floc'h, E., Fabri, M.C., Sarradin, P.M., Sarrazin, J., 2012. Biological data extraction from imagery - how far can we go? A case study from the Mid-Atlantic Ridge. Mar. Environ. Res. 82, 15–27. https://doi.org/10.1016/j.marenvres.2012.09.001.

Davies, J.S., Guillaumont, B., Tempera, F., Vertino, A., Beuck, L., Ólafsdóttir, S.H., Smith, C.J., Fosså, J.H., van den Beld, I.M.J., Savini, A., Rengstorf, A., Bayle, C., Bourillet, J.F., Arnaud-Haond, S., Grehan, A., 2017. A new classification scheme of European cold-water coral habitats: implications for ecosystem-based management of the deep sea. Deep. Res. Part II Top. Stud. Oceanogr. 145, 102–109. https://doi.org/10.1016/j.dsr2.2017.04.014.

Davies, J.S., Stewart, H.A., Narayanaswamy, B.E., Jacobs, C., Spicer, J., Golding, N., Howell, K.L., 2015. Benthic assemblages of the Anton Dohrn Seamount (NE Atlantic): defining deep-sea biotopes to support habitat mapping and management efforts with a focus on vulnerable marine ecosystems. PLoS One 10, e0124815. https://doi.org/10.1371/journal.pone.0124815.

De la Torriente, A., Serrano, A., Fernández-Salas, L.M., García, M., Aguilar, R., 2018. Identifying epibenthic habitats on the Seco de los Olivos Seamount: species assemblages and environmental characteristics. Deep. Res. Part I Oceanogr. Res. Pap. 135, 9–22. https://doi.org/10.1016/j.dsr.2018.03.015.

Ferrari, R., McKinnon, D., He, H., Smith, R.N., Corke, P., González-Rivero, M., Mumby, P. J., Upcroft, B., 2016. Quantifying multiscale habitat structural complexity: a cost-effective framework for underwater 3D modelling. Rem. Sens. https://doi.org/10.3390/rs8020113.

Freiwald, A., 2011. Cold-water coral reefs. In: Encyclopedia of Earth Sciences Series. Springer, Netherlands, pp. 225–229. https://doi.org/10.1007/978-90-481-2639-2_68.

García-Alegre, A., Sánchez, F., Gómez-Ballesteros, M., Hinz, H., Serrano, A., Parra, S., 2014. Modelling and mapping the local distribution of representative species on the le danois bank, El cachucho marine protected area (cantabrian sea). Deep. Res. Part II Top. Stud. Oceanogr. 106, 151–164. https://doi.org/10.1016/j.dsr2.2013.12.012.

Gomes-Pereira, J.N., Carmo, V., Catarino, D., Jakobsen, J., Alvarez, H., Aguilar, R., Hart, J., Giacomello, E., Menezes, G., Stefanni, S., Colaço, A., Morato, T., Santos, R. S., Tempera, F., Porteiro, F., 2017. Cold-water corals and large hydrozoans provide essential fish habitat for Lappanella fasciata and Benthocometes robustus. Deep. Res. Part II Top. Stud. Oceanogr. 145, 33–48. https://doi.org/10.1016/j.dsr2.2017.09.015.

Guillou, H., Carracedo, J.C., Pérez Torrado, F., Rodriguez Badiola, E., 1996. K-Ar ages and magnetic stratigraphy of a hotspot-induced, fast grown oceanic island: El Hierro, Canary Islands. J. Volcanol. Geoth. Res. 73, 141–155. https://doi.org/10.1016/0377-0273(96)00021-2.

Guisan, A., Zimmermann, N.E., 2000. Predictive habitat distribution models in ecology. Ecol. Model. 135, 147–186.

Harris, P.T., Baker, E.K., 2012. Why map benthic habitats?. In: Seafloor Geomorphology as Benthic Habitat https://doi.org/10.1016/B978-0-12-385140-6.00001-3.

He, H., Ferrari, R., McKinnon, D., Roff, G., Mumby, P., Smith, R., Upcroft, B., 2012. Measuring reef complexity and rugosity from monocular video bathymetric reconstruction. In: 12th International Coral Reef Symposium. ICRS, 2012.

IEO, 2013. Caracterización del Banco de La Concepción. Informe del Instituto español de Oceanografía - Centro Oceanográfico de Canarias, Madrid.

Kahn, A.S., Ruhl, H.A., Smith, K.L., 2012. Temporal changes in deep-sea sponge populations are correlated to changes in surface climate and food supply. Deep-Sea Res. Part I Oceanogr. Res. Pap. 70, 36–41. https://doi.org/10.1016/J.DSR.2012.08.001.

Kassambara, A., 2020. Ggpubr. ggplot2" Based Publication Ready Plots.

Kazanidis, G., Vad, J., Henry, L.A., Neat, F., Berx, B., Georgoulas, K., Roberts, J.M., 2019. Distribution of deep-sea sponge aggregations in an area of multisectoral activities and changing oceanic conditions. Front. Mar. Sci. 6, 163. https://doi.org/10.3389/FMARS.2019.00163/BIBTEX.

Kenchington, E., Murillo, F.J., Lirette, C., Sacau, M., Koen-Alonso, M., Kenny, A., Ollerhead, N., Wareham, V., Beazley, L., 2014. Kernel density surface modelling as a means to identify significant concentrations of vulnerable marine ecosystem indicators. PLoS One 9, e109365. https://doi.org/10.1371/journal.pone.0109365.

Lawrence, M.A., 2016. Ez: easy analysis and visualization of factorial experiments. R Packag. version 4.4-0.

Leon, J.X., Roelfsema, C.M., Saunders, M.I., Phinn, S.R., 2015. Measuring coral reef terrain roughness using "Structure-from-Motion" close-range photogrammetry. Geomorphology. https://doi.org/10.1016/j.geomorph.2015.01.030.

Leys, S.P., Lauzon, N.R.J., 1998. Hexactinellid sponge ecology: growth rates and seasonality in deep water sponges. J. Exp. Mar. Biol. Ecol. 230, 111–129. https://doi.org/10.1016/S0022-0981(98)00088-4.

Mistri, M., 1995. Gross morphometric relationships and growth in the mediterranean gorgonian paramuricea clavata. Bolletino di Zool 62, 5–8. https://doi.org/10.1080/11250009509356043.

Ninio, R., Delean, S., Osborne, K., Sweatman, H., 2003. Estimating cover of benthic organisms from underwater video images: variability associated with multiple observers. Mar. Ecol. Prog. Ser. 265, 107–116. https://doi.org/10.3354/meps265107.

Olinger, L.K., Scott, A.R., McMurray, S.E., Pawlik, J.R., 2019. Growth estimates of Caribbean reef sponges on a shipwreck using 3D photogrammetry. Sci. Rep. https://doi.org/10.1038/s41598-019-54681-2.

OSPAR, 2010. Background Document for Deep-Sea Sponge Aggregations. Biodiversity Series.

OSPAR, 2008. List of Threatened And/or Declining Species and Habitats (Reference Number: 2008-6). London.

Pajuelo, J.G., Seoane, J., Biscoito, M., Freitas, M., González, J.A., 2016. Assemblages of deep-sea fishes on the middle slope off Northwest Africa (26°–33° N, eastern Atlantic). Deep. Res. Part I Oceanogr. Res. Pap. 118, 66–83. https://doi.org/10.1016/j.dsr.2016.10.011.

Palma, M., Casado, M., Pantaleo, U., Pavoni, G., Pica, D., Cerrano, C., 2018. SfM-based method to assess gorgonian forests (paramuricea clavata (Cnidaria, octocorallia)). Rem. Sens. 10, 1154. https://doi.org/10.3390/rs10071154.

Prado, E., Cristobo, J., Rodríguez-Basalo, A., Ríos, P., Rodríguez-Cabello, C., Sánchez, F., 2021. In situ growth rate assessment of the hexactinellid sponge Asconema setubalense using 3D photogrammetric reconstruction. Front. Mar. Sci. 8, 26. https://doi.org/10.3389/fmars.2021.612613.

Prado, E., Sánchez, F., Rodríguez-Basalo, A., Altuna, A., Cobo, A., 2019a. Semi-automatic method of fan surface assessment to achieve gorgonian population structure in Le Danois Bank, Cantabrian Sea. In: ISPRS Annals of the Photogrammetry, Remote Sensing and Spatial Information Sciences, pp. 167–173. https://doi.org/10.5194/isprs-archives-XLII-2-W10-167-2019. Copernicus GmbH.

Prado, E., Sánchez, F., Rodríguez-Basalo, A., Altuna, Á., Cobo, A., 2019b. Analysis of the population structure of a gorgonian forest (Placogorgia sp.) using a photogrammetric 3D modeling approach at Le Danois Bank, Cantabrian Sea. Deep. Res. Part I Oceanogr. Res. Pap. 153 https://doi.org/10.1016/j.dsr.2019.103124.

Price, D.M., Robert, K., Callaway, A., Lo Iacono, C., Hall, R.A., Huvenne, V.A.I., 2019. Using 3D photogrammetry from ROV video to quantify cold-water coral reef structural complexity and investigate its influence on biodiversity and community assemblage. Coral Reefs. https://doi.org/10.1007/s00338-019-01827-3.

Prouty, N.G., Roark, E.B., Buster, N.A., Ross, S.W., 2011. Growth rate and age distribution of deep-sea black corals in the Gulf of Mexico. Mar. Ecol. Prog. Ser. 423, 101–115. https://doi.org/10.3354/meps08953.

Pusceddu, A., Bianchelli, S., Martín, J., Puig, P., Palanques, A., Masqué, P., Danovaro, R., 2014. Chronic and intensive bottom trawling impairs deep-sea biodiversity and ecosystem functioning. Proc. Natl. Acad. Sci. U.S.A. 111, 8861–8866. https://doi.org/10.1073/pnas.1405454111.

R Core Team, 2020. R: A Language and Environment for Statistical Computing.

Ramiro-Sánchez, B., González-Irusta, J.M., Henry, L.-A., Cleland, J., Yeo, I., Xavier, J.R., Carreiro-Silva, M., Sampaio, Í., Spearman, J., Victorero, L., Messing, C.G., Kazanidis, G., Roberts, J.M., Murton, B., 2019. Characterization and mapping of a deep-sea sponge ground on the tropic seamount (northeast tropical atlantic): implications for spatial management in the high seas. Front. Mar. Sci. 6 https://doi.org/10.3389/fmars.2019.00278.

Rivera, J., Canals, M., Lastras, G., Hermida, N., Amblas, D., Arrese, B., Martín-Sosa, P., Acosta, J., 2016. Morphometry of concepcion bank: evidence of geological and biological processes on a large volcanic seamount of the canary islands seamount Province. PLoS One. https://doi.org/10.1371/journal.pone.0156337.

Rudis, B., 2020. Hrbrthemes: Additional Themes, Theme Components and Utilities for "Ggplot2.

Sánchez, F., Rodríguez Basalo, A., García-Alegre, A., Gómez-Ballesteros, M., 2017. Hard-bottom bathyal habitats and keystone epibenthic species on le danois bank (cantabrian sea). J. Sea Res. 130, 134–153. https://doi.org/10.1016/j.seares.2017.09.005.

Sánchez, F., Serrano, A., Ballesteros, M.G., 2009. Photogrammetric quantitative study of habitat and benthic communities of deep Cantabrian Sea hard grounds. Continent. Shelf Res. 29, 1174–1188. https://doi.org/10.1016/j.csr.2009.01.004.

Santín, A., Grinyó, J., Ambroso, S., Uriz, M.J., Dominguez-Carrió, C., Gili, J.M., 2019. Distribution patterns and demographic trends of demosponges at the menorca channel (northwestern mediterranean sea). https://doi.org/10.1016/j.pocean.2019.02.002.

Schneider, C.A., Rasband, W.S., Eliceiri, K.W., 2012. NIH Image to ImageJ: 25 years of image analysis. Nat. Methods 97 (9), 671–675. https://doi.org/10.1038/nmeth.2089, 2012.

Serrano, A., Cartes, J.E., Papiol, V., Punzón, A., García-Alegre, A., Arronte, J.C., Ríos, P., Lourido, A., Frutos, I., Blanco, M., 2017a. Epibenthic communities of sedimentary habitats in a NE Atlantic deep seamount (Galicia Bank). J. Sea Res. 130, 154–165. https://doi.org/10.1016/j.seares.2017.03.004.

Serrano, A., González-Irusta, J.M., Punzón, A., García-Alegre, A., Lourido, A., Ríos, P., Blanco, M., Gómez-Ballesteros, M., Druet, M., Cristobo, J., Cartes, J.E., 2017b. Deep-sea benthic habitats modeling and mapping in a NE Atlantic seamount (Galicia Bank). Deep. Res. Part I Oceanogr. Res. Pap. 126, 115–127. https://doi.org/10.1016/j.dsr.2017.06.003.

Sitjà, C., Maldonado, M., Farias, C., Rueda, J.L., 2019. Deep-water sponge fauna from the mud volcanoes of the gulf of cadiz (North Atlantic, Spain). J. Mar. Biol. Assoc. U. K. 99, 807–831. https://doi.org/10.1017/S0025315418000589.

Spalding, M.D., Fox, H.E., Allen, G.R., Davidson, N., Ferdaña, Z.A., Finlayson, M., Halpern, B.S., Jorge, M.A., Lombana, A., Lourie, S.A., Martin, K.D., McManus, E., Molnar, J., Recchia, C.A., Robertson, J., 2007. Marine ecoregions of the world: a bioregionalization of coastal and shelf areas. Bioscience 57, 573–583. https://doi.org/10.1641/B570707.

Tabachnick, K.R., 2002. Family Rossellidae schulze, 1885. Syst. Porifera 1441–1505. https://doi.org/10.1007/978-1-4615-0747-5_148.

Tabachnick, K.R., Menshenina, L.L., 2007. Revision of the genus Asconema (Porifera: hexactinellida: Rossellidae). J. Mar. Biol. Assoc. U. K. 87, 1403–1429. https://doi.org/10.1017/S0025315407058158.

Tola, E., Lepetit, V., Fua, P., 2010. DAISY: an efficient dense descriptor applied to wide-baseline stereo. IEEE Trans. Pattern Anal. Mach. Intell. 32, 815–830. https://doi.org/10.1109/TPAMI.2009.77.

Van Den Bogaard, P., 2013. The origin of the Canary Island Seamount Province-New ages of old seamounts. Sci. Rep. 3, 1–7. https://doi.org/10.1038/srep02107.

Victorero, L., Watling, L., Deng Palomares, M.L., Nouvian, C., 2018. Out of sight, but within reach: a global history of bottom-trawled deep-sea fisheries from >400 m depth. Front. Mar. Sci. 5, 98. https://doi.org/10.3389/fmars.2018.00098.

VideoLan, 2006. VLC Media Player.

Weigel, W., Goldflam, P., Hinz, K., 1978. The crustal structure of the conception bank. Mar. Geophys. Res. 3, 381–392.

Wickham, H., 2016. ggplot2: Elegant Graphics for Data Analysis.

Wood, S.N., 2017. Generalized Additive Models: an Introduction with R, second ed.

Young, G.C., Dey, S., Rogers, A.D., Exton, D., 2018. Correction: cost and time-effective method for multi-scale measures of rugosity, fractal dimension, and vector dispersion from coral reef 3D models, 2018 PLoS One 12, e0175341. https://doi.org/10.1371/journal.pone.0201847, 10.1371/journal.pone.0175341). PLoS One.